Journal of Water Process Engineering 45 (2022) 102515

Contents lists available at ScienceDirect

Journal of Water Process Engineering

journal homepage: www.elsevier.com/locate/jwpe

Prototyping a spinning adsorber submerged filter for continuous removal of wastewater contaminants

José María Obón *, José Manuel Angosto, Francisco González-Soto, Aldana Ascua, José Antonio Fernández-López

Departamento de Ingeniería Química y Ambiental, Universidad Politécnica de Cartagena, Spain

ARTICLE INFO

Keywords:
Spinning adsorber
Submerged filter
Active carbon
Azorubine
Wastewater contaminants
Wastewater treatment

ABSTRACT

Adsorption process is widely used for the removal of wastewater contaminants. Classic adsorption units are fixed beds and membrane filtration systems. In this work a novel configuration of a bench scale spinning adsorber submerged filter is proposed. Different prototypes of cylindric, truncated cone or prismatic spinning adsorbers were studied using activated carbon of different particle sizes GAC (1.5 mm, Granulated), μGAC (0.475 mm, microGranulated), and cPAC (0.237 mm, coarse Powder) as adsorbent, and azorubine as model adsorbate. High maximum azorubine adsorptions per unit mass of adsorbent of 214, 225 and 275 mg/g for GAC, μGAC and cPAC, respectively, were obtained using the Langmuir isotherm adsorption model. Batch adsorption followed pseudo-second order kinetics, and adsorbate uptake rate increased with decreasing adsorbent particle size. Best adsorption unit was a tank equipped with a spinning rectangular prism adsorber prototype all made of stainless-steel woven wire filter of 180 mesh size. Running at 600 rpm and filled with a high cPAC concentration (25 g/L), adsorber can remove azorubine at similar rates that the use of free moving cPAC. Adsorber unit can run in continuous mode and works even better as a novel spinning submerged filter where filtered flow exits from a central pipe axis. This integrated adsorption-submerged filtration operation mode offer the possibility of adding a high initial dose or a continuous dosing of adsorbent in the tank, increasing the adsorbent concentration of the unit. This system can also offer novel opportunities for wastewater contaminants removal using different adsorbent materials located separately.

1. Introduction

Water cleaning is a key objective and challenge essential to human health, social and economic development. Presence in aquatic environments of contaminants and nowadays emerging contaminants is receiving increasing interest in governments, due to their undesirable effects on ecosystems and humans. An example of contaminants are industrial dyes and their by-products that are carcinogenic and toxic [1]. Other water-soluble contaminants of high concern include pharmaceuticals, daily personal care products, endocrine-disrupting chemicals, hormones, pesticides, biocides, organic chemicals, or heavy metals [2,3].

Wastewater treatments plants should act as primary barriers against the spread of contaminants because wastewaters can be considered as a central source of this pollution. It must be done an effort in treatments to remove all the contaminants present both in industrial and domestic wastewaters where contaminant concentrations may vary from mg/L to ng/L. Conventional physico-chemical and biological procedures have poor removal efficiency for recalcitrant compounds so additional techniques after conventional wastewater treatments plants are needed to avoid its discharge to the aquatic environment [4,5]. Important removal technologies applicable for dye or micropollutants removal from wastewaters are adsorption or membrane processes, followed by biological treatments or advanced oxidation processes [6–8]. Sometimes, hybrid systems combining different technologies can enhance removal efficiency for many types of contaminants [9,10].

The most extended and well-known treatment technology at full-scale plants for contaminants removal is adsorption [11]. This technique can use a broad range of materials to adsorb the high variety of contaminants present in wastewaters. The great assortment of adsorbent materials includes not only classic activated carbon from mineral or vegetal sources, but also bioadsorbents from biomass residues, inorganic

* Corresponding author at: Departamento de Ingeniería Química y Ambiental, Universidad Politécnica de Cartagena, Paseo Alfonso XIII, 52, E-30203 Cartagena, Murcia, Spain.

E-mail addresses: josemaria.obon@upct.es (J.M. Obón), jm.angosto@upct.es (J.M. Angosto), josea.fernandez@upct.es (J.A. Fernández-López).

https://doi.org/10.1016/j.jwpe.2021.102515
Received 21 October 2021; Received in revised form 19 November 2021; Accepted 10 December 2021
Available online 23 December 2021

materials, nanoadsorbents or novel multifunctional materials that combine adsorption with photocatalysis or antibacterial properties [12–15]. Activated carbon (AC) is the most extensively used adsorbent, because its structure offers very high surface areas (>3000 m^2/g), high porosity, and high degree of surface interactions. The available AC forms vary on average particle diameter sizes from >0.25 mm of granulated activated carbon (GAC), to <0.25 mm for powder activated carbon (PAC). Furthermore, according with pore diameters AC is classified as macroporous (≥50 nm), mesoporous (50–2 nm), and microporous (≤2 nm). Mesopores are suitable for large to medium organic molecules (colour, taste, and odour) and micropores for smaller micropollutants [16]. Advantages of adsorption treatments are that no toxic compounds are formed, it has high effectiveness (also at low contaminant concentrations), good cost-efficiency, flexibility in design and operation, and feasible regeneration. However, special attention should be paid for reusability or proper disposal of saturated adsorbents, and the competitive adsorption in presence of dissolved organic matter [17].

Classic adsorption units for contaminants removal are GAC adsorbers of the fixed bed type and can be conventional rapid gravity or more commonly, pressure filters. Empty bed contact times (EBCT) varies for different micropollutants, and it is usually in the range 5–30 min [18]. Although PAC has a larger available specific surface area resulting in faster adsorption kinetics, its use in fixed beds is limited because of its high compaction. The use of PAC can be extended as a tertiary treatment by the implementation of an additional separation process like sedimentation or filtration. Thus, PAC can be directly feed as a powdered slurry at the inlet to the treatment plant, and later removed with clarifier sludge. Selection between GAC and PAC competes because of the advantages of both [19]. Continuous submerged membrane filtration coupled with PAC has been also applied for micropollutants removal from wastewaters [20].

Another possibility not applied in full scale wastewater treatment plants is the use of rotating adsorbers. A first option is rotating packed bed contactors where liquid enters through the centre of a doughnut shaped packed bed adsorber that rotate at high speeds generating high gravity centrifugal forces [21]. A second option is rotating adsorbers built with spinning baskets filled with adsorbent, which works as impellers inside the adsorption tank. Up to known diverse designs has been tested with different cylindrical perforated baskets dispositions, and CFD models have been implemented for descriptions of internal mixing [22,23]. These configurations facilitate an efficient adsorption process by particle movement, minimizing external and intraparticular adsorbate diffusional problems, and improving the use of porous activated carbons. If we compare continuous operation of these rotating basket adsorbers with packed beds it must be considered that rotating adsorbers work with lower adsorbent concentrations, because volume located outside rotating baskets has no adsorbent. It means that continuous spinning adsorbers should use adsorbents with high adsorption capacity and fast kinetics to be viable in full scale plants. An advantage of these adsorber units versus packed beds is its easy pH control.

This study explores a novel versatile prototype of spinning adsorber for wastewater contaminants removal. The new prototype proposal can work both with the standard adsorbent inside of the spinning basket adsorber and as a spinning submerged filter with the adsorbent located outside. This second continuous operation mode as a submerged filter can take advantage of a higher adsorbent concentration with the possibility of fresh adsorbent addition with time. Different spinning adsorber geometric configurations were studied within a variety of cylindric, truncated cone or prismatic baskets prototypes made with mesh of different sizes. Impeller configurations tested generate different axial or radial flows in the tank. Adsorption was studied using activated carbon of different particle sizes (GAC, μGAC and PAC) to estimate the best particle size for operation. It is expected that small particles will offer higher specific surface areas and faster adsorption kinetics, but favour compaction. A high micropore volume activated carbon was selected as adsorbent to evaluate a condition with high mass transfer limitations. The adsorbate used in this study was azorubine, an azo acid dye contaminant from textile industry. Azorubine is also present at high concentrations in pharmaceutical and mouthwash compositions as excipient, and it is a potential emerging contaminant. Azorubine was selected as adsorbate because it is high water-soluble, stable to pH, heat, and light, and has well-known adsorption kinetics in activated carbon. Experiments evaluate the effect of activated carbon concentration, particle size, and rotation speed on adsorption kinetics in batch spinning adsorbers. Finally, continuous adsorption studies compare the operation mode where flow exits directly from the tank, and a novel adsorption-submerged filtration operation mode where flow exits from the central tube axis once filtered. This unit is a new proposal that could be used in wastewater treatment plants for contaminants removal.

2. Materials and methods

2.1. Materials

The adsorbent used in this study was extrapure granular activated carbon (GAC) 1.5 mm particle diameter from MERCK (ref. 102514, Darmstadt, Germany). The adsorbate was azorubine (Acid Red 14, Food Red 3, carmoisine, CI. 14720) of 85% purity (Fiorio Colori S.p.a., Gessate, Italia). Acetone, ethanol 96%, hydrochloric acid (37%), sodium hydroxide, potassium nitrate, and phenolphthalein were from Sigma-Aldrich (Madrid, Spain). Water was deionized with an Elix Essential 3 equipment (Merck, Madrid, Spain).

2.2. Prototypes of spinning adsorbers

Two different spinning adsorber prototypes were proposed, labelled as A and B. Fig. 1 shows the first option A that offers a radial flow pattern. It consists of a 2 L glass beaker with a water jacket, thermostated at 25 °C with a circulating water bath (Lauda, Königshofen, Germany). Inside the glass beaker rotate an impeller shaft built with two baskets hold to a metallic bar. Two different basket designs are used: plastic baskets with frontal filter mesh, or metallic baskets all made of filter mesh. In addition, studied baskets have two geometries: cylindric or truncated cone. Plastic baskets were made with a rapid Prototyping 3D printer (Dimension BST 1200es, Stratasys, USA). This technology print from the 3D solid model generated in the CAD system. Plastic material was ABS plus. Metallic baskets were made of stainless-steel woven wire filter from the development of its surface and glued with cyanoacrylate adhesive. In all cases, activated carbon was weight, placed inside the baskets, and two circular lids made with filters of the different mesh sizes studied were located at both ends to avoid adsorbent lost. Stainless-steel woven wire filters were supplied with different mesh sizes: mesh 35, 100 (Comercial García, Molina del Segura, Spain) and 180 (GIIH, Amazon, Spain), of 0.50, 0.15, and 0.085 mm mesh hole size, respectively. Basket volumes ranged between 8 and 12 mL. The second prototype option B is shown in Fig. 2 and offers an axial flow pattern instead. It is like the first option but use a 0.25 L glass beaker with a water jacket and a configuration with only one rectangular prismatic plastic basket covered with stainless-steel filters. Tank was equipped with four equally spaced baffles necessary to work with rotational speeds higher than 200 rpm. In all cases impellers were placed at a height of one third of the diameter of the tank from the bottom and rotated with an overhead stirrer Microstar 7.5 digital (IKA-Werke GmbH & Co., Staufen, Germany).

2.3. Mixing time experiments

Studies were done with all designed prototypes made with stainless steel woven wire filter of mesh 35, and empty. Results were compared with the stirring of a flat blade impeller (Fig. 1). Mixing time was measured as the time it takes for the disappearance of the pink colour of

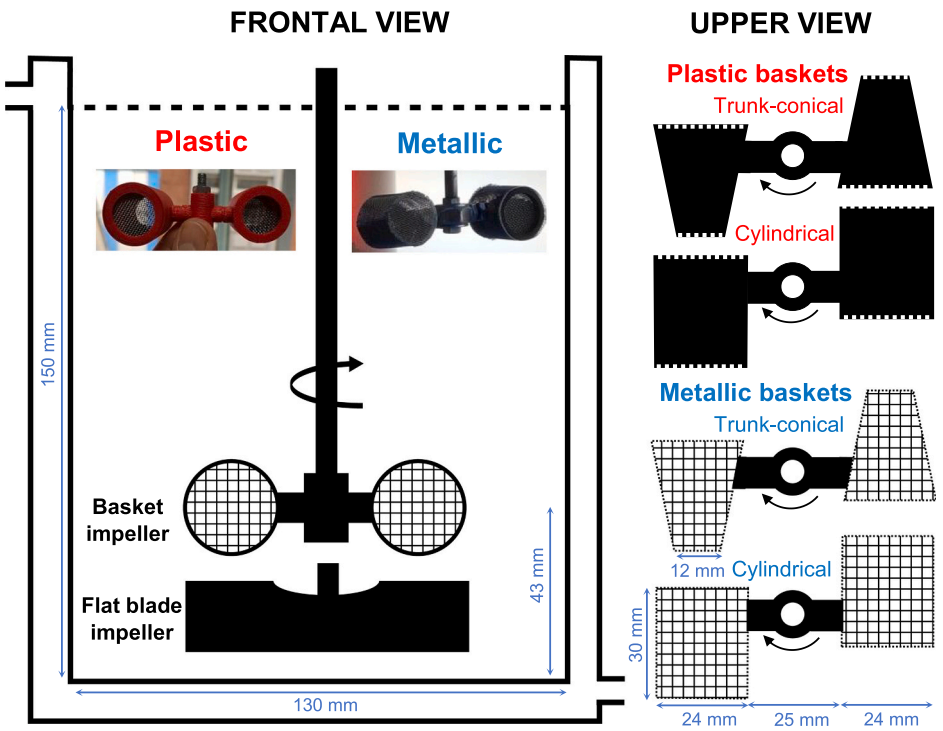

Fig. 1. Illustration of spinning adsorber prototypes with radial flow (Type A) showing the studied plastic and metallic basket configurations: cylindrical or trunk conical.

the phenolphthalein indicator in a dilute sodium hydroxide solution by adding an excess of hydrochloric acid [24]. Tests were carried out filling the tank with deionized water, 1 mL of 2 M NaOH solution, and 1 mL of phenolphthalein solution (0.5% in ethanol). The stirrer device is then turned on at the speed to be tested, and pink colour is evenly distributed. Then 1 mL of 3 M hydrochloric acid is added by means of a micropipette at a fixed point in the upper part of the tank. A mobile phone is placed in front of the tank and a video is started at the same time as the acid is added. The mixing time is determined when no colour is observed after viewing the video. A Jar Test and Leaching Test Type FC 6S with six agitation units was used to study rotation speeds from 10 to 200 rpm (Velp Scientifica Srl, Usmate, Italia). Tests were carried out in triplicate.

2.4. Obtention of activated carbons with different granulometry (μGAC, cPAC and PAC)

Different granulometries were obtained from commercial 1.5 mm GAC after different dry grinding techniques and sieving. GAC (Granular Activated Carbon) was milled with a grinder using the customized grinding option at the minimum value (GVX242 Krups, SEB Group, Spain). Fraction of particles collected between stainless steel 0.85–0.25 mm sieves (FiltraVibración S.L, Barcelona, Spain) were labelled as μGAC (microGranular Activated Carbon), and those between 0.25 and 0.100 mm sieves were labelled as cPAC (coarse Powder Activated Carbon). GAC was also milled with an IKA MF 10 basic mill equipped with MF 10.1 cut grinding head and a 0.25 mm curved separation screen (IKA-Werke, Staufen, Germany). Then, particles were sieved with a stainless steel 0.1 mm sieve, and filtered fraction was labelled as PAC (Powder Activated Carbon).

2.5. Physical characterization of activated carbons

Particle size characterization of activated carbons was carried out by laser diffraction with a Mastersizer 2000 S equipped with a "Hydro 2000G" unit (Malvern Instruments Ltd., UK). Samples were added to reach the proper obscuration range and then measurements made in triplicate.

Specific surface area of the activated carbons was measured using adsorption-desorption isotherms of N_2 at 77 K and CO_2 at 273 K using an Autosorb iQ XR-2 automated gas sorption analyzer (Quantachrome Instruments, Boynton Beach, Florida). Prior to the gas adsorption measurements, samples were degassed at 250 °C for 4 h. Total surface areas were determined from desorption isotherms of N_2 using the multipoint Brunauer–Emmett–Teller (BET) method, total pore volume obtained as P/P_0 0.95, and micro (<2 nm) and ultramicropores (<0.7 nm) volume according with Dubinin-Radushkevic model from desorption isotherms of N_2 and CO_2, respectively [25].

True density of activated carbon was measured with a pycnometer (VidraFOC S.A., Barcelona, Spain). Apparent density was quantified as the weight of activated carbon that filled a 10 ml cylinder, measured with a 4-digit precision electronic balance AX224 (Sartorius AG, Goettingen, Germany). In the case of compact or tapped density the weight of activated carbon that filled a 10 mL cylinder was compacted with small strokes until the volume remained constant (after approximately 1500 taps) (Autotap, Quantachrome, USA). In all cases, the density values were calculated as the weight in grams divided by the volume occupied by the sample. Measurements were made in triplicate.

The pH at the point zero charge (pH_{PZC}) was determined according with the mass titration method, putting into contact activated carbons within the concentration range 5–100 g/L with 50 mL of a 0.03 M KNO_3 solution. Flasks were agitated for 24 h in a shaker at 250 rpm until equilibrium pH was reached. The pH_{PZC} was calculated as the pH at which a plateau is achieved when plotting equilibrium pH versus activated carbon concentrations [26].

2.6. Batch adsorption isotherm studies

Adsorption isotherms of azorubine on activated carbon were obtained mixing in 100 mL flasks 25 ml of different azorubine concentrations (50–500 mg/L) and 12.5 mg of an activated carbon (GAC, μGAC, cPAC). pH of azorubine solutions were fixed to 7.0, simulating pH of wastewater effluents that are neutralized during pretreatment. Flasks

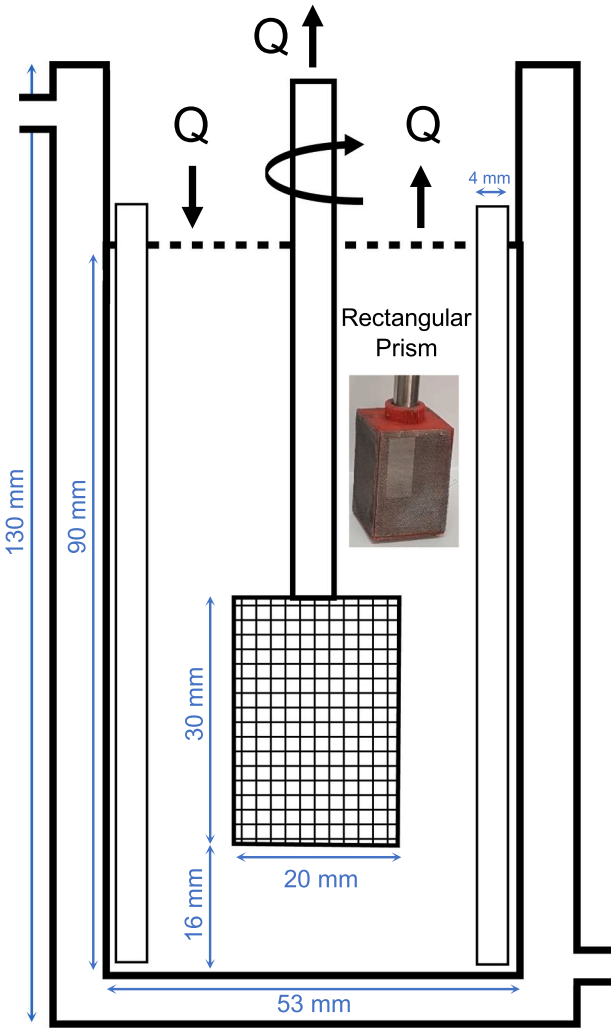

Fig. 2. Illustration of spinning adsorber prototype with axial flow (Type B) showing the rectangular prismatic basket impeller.

were thermostated at 25 °C in a dark chamber, and orbitally shaken at 200 rpm. After 5 days equilibrium was reached, then 2 mL samples were withdrawn and filtered with 0.45 μm disposable syringe filters of regenerated cellulose (Agilent, Germany) to remove any carbon particle. Finally, azorubine samples were diluted with deionized water, and its absorbance measured at 516 nm versus a blank cell filled with distilled water using an Agilent 8453 (Waldbronn, Germany). Azorubine concentrations were calculated from absorbance values bellow 1 AU through the calibration curve of absorbance versus azorubine concentration (mg/L), which slope was 0.0492. Coefficient of determination (r^2) of simple linear regression was 0.9992.

The amount of azorubine adsorbed per mass of adsorbent (mg/g) was quantified by:

$$q_e = (C_o - C_e)\ V/W \tag{1}$$

where C_0 is the initial concentration of azorubine in the solution (mg/L), C_e is the concentration in the solution once the adsorption process reached equilibrium, V is the volume of the solution (0.025 L), and W is the adsorbent dosage (0.0125 g). Adsorbent concentration is 0.5 g/L.

Values of q_e versus C_e were adjusted to different models of adsorption isotherms such as Langmuir (Eqs. (2), (3)) and Freundlich (Eq. (4)) [27].

$$q_e = q_{max}\frac{K_L}{1 + K_L C_e} \tag{2}$$

$$R_L = \frac{1}{1 + K_L\ C_0} \tag{3}$$

$$q_e = K_F\ C_e^{1/n} \tag{4}$$

An EXCEL sheet and the solver function were used to perform a non-linear regression fit of the data. Error function considered for minimization was coefficient of determination ($r^2 = 1$):

$$r^2 = \frac{\sum_{i=1}^{n}\left(q_{e,exp} - \overline{q}_{e,cal}\right)_i^2}{\sum_{i=1}^{n}\left(q_{e,exp} - \overline{q}_{e,cal}\right)_i^2 + \sum_{i=1}^{n}\left(q_{e,exp} - q_{e,cal}\right)_i^2} \tag{5}$$

where $q_{e,\ exp}$ is the azorubine adsorbed per unit mass of adsorbent (mg/g), $q_{e,\ cal}$ is the azorubine adsorbed per unit mass of adsorbent obtained with the adjustment to the model (mg/g), $\overline{q}_{e,cal}$ is the mean of $q_{e,\ cal}$, and n is the number of experimental data [27,28].

2.7. Batch adsorption kinetic studies

Kinetic adsorption of azorubine were studied at 25 °C both with activated carbons in free form or with the spinning adsorbers prototypes filled with activated carbons (GAC, μGAC or cPAC) using concentrations from 2 to 25 g/L. Rotation speeds of spinning adsorbers were studied in the range from 200 to 600 rpm. Tanks were filled with azorubine concentrations ranging from 34 to 510 mg/L (pH 7.0), depending on activated carbon concentration used. In all cases samples were withdrawn of the tanks at the necessary time intervals to follow the adsorption process, filtered if needed with 0.45 μm disposable syringe filters, its absorbance at 516 nm determined, and finally the azorubine concentration calculated.

The amount of azorubine adsorbed per mass of adsorbent (mg/g) was quantified by:

$$q_t = (C_o - C_t)\ V/W \tag{6}$$

where C_o is the initial concentration of azorubine in the solution (mg/L), C_t is the concentration at time t once the adsorption process has started, V is the volume of the solution and W is the adsorbent dosage.

Values of q_t versus time were adjusted to adsorption reaction models of pseudo-first order (Eq. (7)), pseudo-second order (Eq. (8)), and Elovich (Eq. (9)), assuming that the overall rate of adsorption is controlled by the adsorption rate of azorubine on the activated carbon surface.

$$q_t = q_e\left(1 - e^{-k_1 t}\right) \tag{7}$$

$$q_e = \frac{k_2\ q_e^2\ t}{1 + k_2\ q_e\ t} \tag{8}$$

$$q_t = (1/\beta)\ ln(\beta\ \alpha\ t) \tag{9}$$

With pseudo-second order kinetic model initial adsorption rate is calculated as $k_2\ q_t^2$ (mg/g min) [29]. Like adsorption isotherm studies, EXCEL and solver were considered for non-linear regression fit of the data using coefficient of determination ($r^2 = 1$) as error function.

To study which is the rate limiting step, film diffusion or intraparticle diffusion, the adsorption diffusion model of Boyd applying the approximations given by Reichenberg was used [30]. According to Boyd's diffusion model intraparticle diffusion is the adsorption rate controlling step when values of Bt plotted versus experimental values of time gives a straight line passing through origin and of B slope. The Boyd number (Bt) was obtained by applying the correspondent equation whether F(t) > 0.85 or F(t) ≤ 0.85:

$$Bt = -Ln\ \frac{\pi^2}{6} - Ln\ (1 - F(t)\ )\ for\ F(t). > 0.85 \tag{10}$$

$$Bt = \left(\sqrt{\pi} - \sqrt{\pi - \frac{\pi^2 F(t)}{3}}\right)^2 \quad for\ F(t) \leq 0.85 \tag{11}$$

For each kinetic data, F(t) can be calculated as q_t/q_e. q_e is the maximum equilibrium concentration. This model also calculates the effective intraparticle diffusion coefficient (Di), known B slope, and the radius of the particle (R) according to the equation:

$$B = \frac{\pi^2 \times D_i}{R^2} \tag{12}$$

2.8. Batch desorption studies: reuse of activated carbon

Studies of azorubine desorption on activated carbon were done with cPAC in a dark chamber thermostated at 25 °C. Initially, 100 mg of cPAC were saturated mixing in 500 mL flasks 100 ml of a 500 mg/L azorubine concentration (pH 7.0). After 5 days agitation at 200 rpm a sample was withdrawn to calculate final azorubine concentration of supernatant, and the amount of azorubine adsorbed quantified as explained previously with Eq. (1). After saturation, supernatant liquid was removed and cPAC used for desorption experiments. Desorption experiments were done in closed vials adding to the 100 mg of saturated cPAC 4 mL of different test solutions: deionized water, 0.1 M HCl (pH 1), 0.1 M NaOH (pH 13), ethanol 96%, or acetone 2, 10, 50 and 90%. cPAC concentration used during desorption was 25 g/L, the maximum concentration than can be achieved in prototype B (Fig. 2). After 2 h of agitation samples were withdrawn, azorubine concentration of supernatant calculated, and the mg of azorubine desorbed quantified multiplying calculated azorubine concentration by added volume (4 mL). Percentage of desorption was calculated as:

$$\%desorption = \frac{mg_{AZ}\ desorbed}{mg_{AZ}\ adsorbed} \times 100 \tag{13}$$

This desorption experiment was repeated different times to achieve a high desorption percentage. Finally, to study the feasibility of adsorbent reuse, desorbed cPAC was saturated once again using 100 ml of a 500 mg/L azorubine concentration (pH 7.0), and the amount of azorubine adsorbed per mass of adsorbent (mg/g) quantified with Eq. (1).

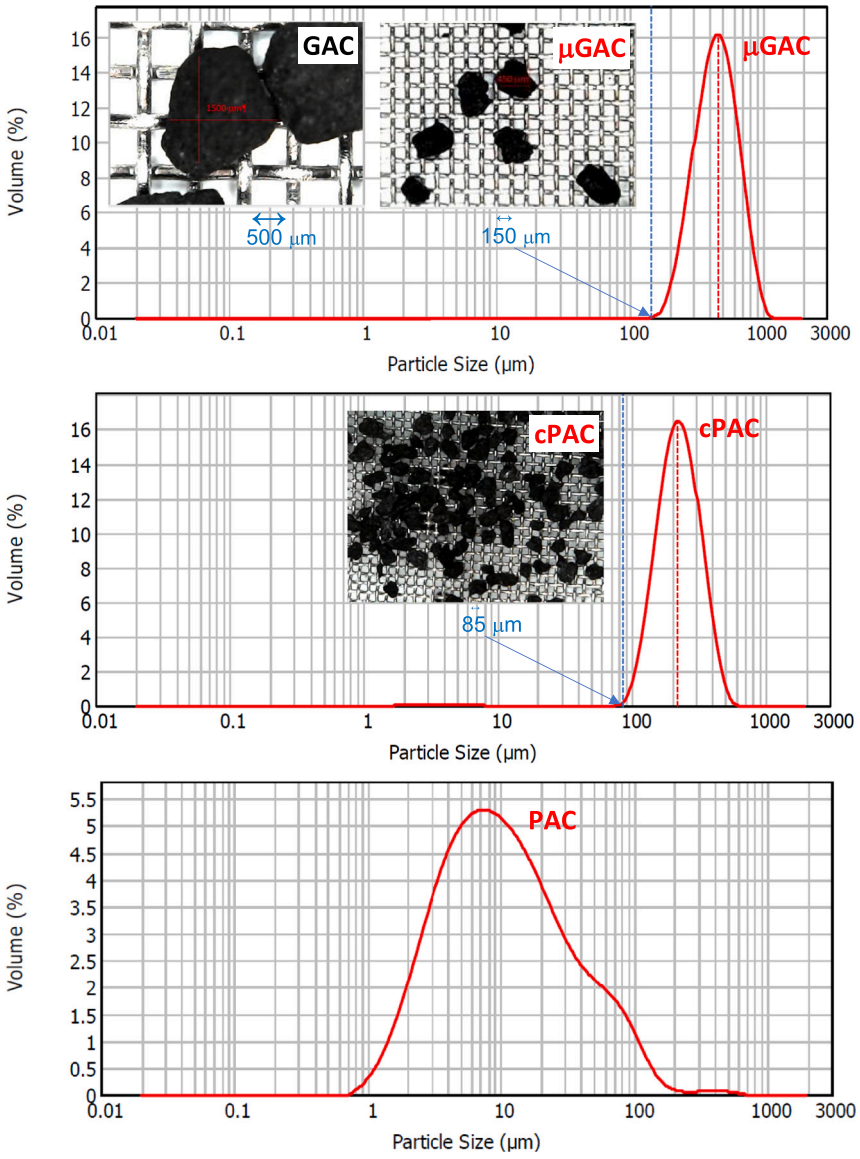

Fig. 3. Particle size distribution curves of µGAC, cPAC and PAC. Inserts compares particle sizes of activated carbons studied with the stainless-steel hole mesh used for particle retention inside spinning adsorbers.

Table 1
Physico-chemical characterization of studied activated carbons.

Parameter	GAC	μGAC	cPAC	PAC
S_{BET} (m^2/g)	942	1014	1078	1206
V_{total} (cm^3/g)	0.492	0.550	0.567	0.669
V_{meso} (cm^3/g)	0.139	0.175	0.078	0.127
V_{micro} (cm^3/g)	0.353	0.375	0.489	0.542
$V_{ultramicro}$ (cm^3/g)	0.268	0.259	0.248	0.242
V_{micro} (%)	72	68	86	81
True density (g/mL)	1.584 ± 0.027	1.597 ± 0.024	1.631 ± 0.031	1.694 ± 0.018
Apparent density (g/mL)	0.484 ± 0.004	0.484 ± 0.006	0.432 ± 0.007	0.320 ± 0.012
Packed density (g/mL)	0.490 ± 0.005	0.502 ± 0.005	0.509 ± 0.003	0.531 ± 0.008
pH_{PZC}	9.8	9.8	9.7	9.7

$S_{BET}(m^2/g)$ = BET surface area
$V_{meso}(cm^3/g)$ = mesopore volume = $V_{total} - V_{micro}$
$V_{ultramicro}(cm^3/g)$ = ultramicropore volume
$V_{total}(cm^3/g)$ = total pore volume
$V_{micro}(cm^3/g)$ = micropore volume
$V_{micro}(\%) = 100 \times V_{micro}/V_{total}$

2.9. Operation in continuous mode with spinning adsorbers

Studies in continuous mode were done using the spinning adsorber prototype option B described in Fig. 2. In all cases 4 g of GAC, μGAC or cPAC were added to the adsorber basket, which means a maximum concentration of 25 g/L in the tank. Experiments were run with a hydraulic retention time of 20 min using an azorubine concentration of 500 mg/L (pH 7.0). Volume level of the tank was kept constant at 160 mL controlling inlet and outlet flows with two peristaltic pumps (Pumpdrive 5001, Heidolph Instruments, Schwabach, Germany). Outlet flow port was located inside the tank, but when the unit run as a spinning submerged filter outlet flow run through the central axis pipe. Adsorption tank was thermostated at 25 °C.

3. Results and discussion

3.1. Obtention and characterization of activated carbons

Commercial granular activated carbon (GAC) of 1.5 mm particle diameter was dry milled to obtain microgranular activated carbon (μGAC), coarse powder activated carbon (cPAC) and powder activated carbon (PAC). Fig. 3 shows measurements of particle size distributions obtained by laser diffraction of μGAC, cPAC and PAC. Curves of μGAC and cPAC are unimodal and quite symmetric. The average particle diameter for μGAC expressed as D[4,3] was 0.475 mm (Span: 0.95, Uniformity: 0.298), for cPAC was 0.237 mm (Span: 0.94, Uniformity: 0.29). PAC particles has a less uniform distribution, a broader span, and the average particle diameter for PAC expressed as D[4,3] was 0.021 mm (Span: 5.13, Uniformity: 1.67). According to the measured average particle sizes, a filter mesh hole size of 0.5 mm was selected to retain GAC inside spinning adsorbers during experimentation, 0.15 mm to retain μGAC, and 0.085 mm to retain cPAC. Inserts of Fig. 3 shows the visual difference in sizes for μGAC and cPAC particles versus filter mesh hole size. It is used a three times lower filter mesh hole size than particle size.

Activated carbons were physically characterized for surface area, porosity, and density (Table 1). GAC commercial activated carbon studied shows high BET surface value (942 m^2/g) and total pore volume (0.492 cm^3/g). These values increase up to 1206 m^2/g and 0.669 cm^3/g for the lower particle size PAC. Activated carbon is mainly microporous as evidenced by the steep adsorption increase at low pressures, however BET adsorption-desorption isotherms showed hysteresis, which indicates the presence of mesopores. The percentage of micropore fraction is quite high with respect to the mesopore amount with values ranging from 68 to 86%. The higher percentages correspond to the lower particle size activated carbons cPAC and PAC. Activated carbons have also a high ultramicroporosity, that decrease slightly with reducing particle size. Obtained values agree with previous characterization of GAC [31,32].

True density values of all activated carbons are higher than apparent density as expected of the porous structure of activated carbons. Apparent density of GAC and μGAC do not change, however cPAC and PAC values are lower because small PAC particles have difficulties to settle. Values of GAC, μGAC and cPAC packed density show a minor increase related with the decrease in particle size, while PAC value is clearly higher which reflect the high compaction degree it can reach. PAC was not studied further because its high compaction level would minimize liquid flow inside spinning adsorbers, and its small particle size do not allow its total retention within the studied adsorbers made of stainless-steel woven wire filter of 0.085 mm mesh hole size.

The pH of zero charge (pH_{PZC}) obtained in this work is 9.7, so surface is positively charged at the pH 7.0 used in this experimentation. This value agrees with surface chemical characterizations found in literature, that also evaluate presence of acid and basic functional groups. Acid substituents are carboxyl, lactone, or phenol groups, while typical basic surface groups are oxygen-containing carbonyls, pyrone and chromene type structures, and oxygen-free Lewis basic sites on the graphene layer. Total acidic and basic surface groups are 0.21 and 0.46 mmol/g GAC, respectively [33]. A correlation of basicity of activated carbon and azorubine adsorption is expected. Previous studies showed that sorption capacity of azorubine although dependent of pH, vary slightly between pH 2 to 6 [34], or pH 5 to 8 [37]. In this work azorubine adsorption was studied in deionized water without buffer addition, so ionic strength is only related to azorubine concentration. The pH of azorubine solutions were adjusted to 7.0 and it was stable during experiments.

GAC has the presence of ionizable groups and a combination of hydrophilic and hydrophobic surface properties. The electrostatic mechanism is not the only mechanism for dye adsorption, GAC has a high affinity for sorbates with phenyl and naphthalene containing groups. Activated carbon can also interact with dye molecules via hydrogen bonding and hydrophobic-hydrophobic mechanisms [34].

3.2. Modelling adsorption isotherms of azorubine on activated carbons

Adsorption isotherms provide a convenient mathematical description to assess the differences in adsorptive capacity of azorubine in GAC, μGAC and cPAC. In this work azorubine adsorption at equilibrium was

Table 2
Modelling parameters of adsorption isotherms.

Model	Parameter	Adsorbent		
		GAC	μGAC	cPAC
Langmuir	q_{max} (mg/g)	214	225	275
	K_L (L/mg)	0.0465	0.0529	0.0821
	R_L	0.04–0.28	0.03–0.26	0.02–0.18
	r^2	0.964	0.958	0.935
Freundlich	K_F ($mg^{(n-1)/n}/g \cdot L^{1/n}$)	55.5	48.5	107.2
	n	4.4	3.8	6.2
	r^2	0.938	0.899	0.983

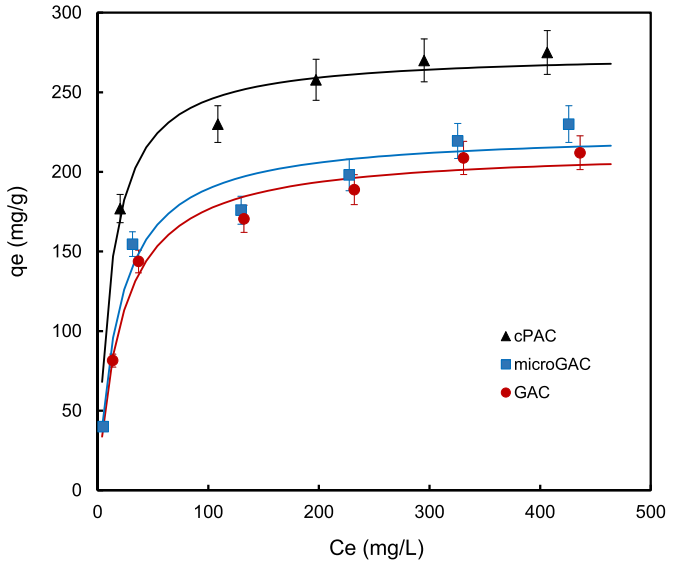

Fig. 4. Adsorption isotherm curves of azorubine on GAC, μGAC, and cPAC fitted with Langmuir model.

Table 3
Modelling parameters of adsorption kinetics.

Model	Parameter	Adsorbent concentration 2 g/L		
		GAC	μGAC	cPAC
Pseudo-first order (Lagergren)	k_1 (1/min)	0.00530	0.02713	0.10313
	q_e (mg/g)	16.61	16.57	16.39
	r^2	0.999	0.999	0.982
Pseudo-second order (Ho)	k_2 (g/mg min)	0.00013	0.00135	0.00827
	q_e (mg/g)	26.82	20.57	18.16
	r^2	0.999	0.996	0.996
Elovich	Alfa (mg/g min)	0.2933	1.1528	11.531
	Beta (g/mg)	0.3152	0.2153	0.3401
	r^2	0.939	0.991	0.954

evaluated with the well-known isotherm models of Langmuir and Freundlich. Table 2 shows the isotherm constants and correlation coefficients (r^2) obtained with the studied models and Fig. 4 the results fitted with Langmuir model. Although both models describe reasonably well the experimental values, Langmuir offered the best description for GAC and μGAC. Previous research with acid dyes showed that Langmuir model fits well experimental values [35,36]. The R_L value indicates favourability of the adsorption process, it is irreversible ($R_L = 0$), favourable ($0 < R_L < 1$), linear ($R_L = 1$), or unfavourable ($R_L > 1$). It can be assumed that azorubine shows a high and favourable adsorption, according to the low values of R_L (0.02–0.28) of Langmuir model. Values of n greater than unity obtained with the model of Freundlich also corroborate favourable adsorption of the dye ($0 > 1/n > 1$). The magnitude of Freundlich constant (K_F) also indicates a high adsorption capacity, which is suitable for the highly heterogeneous surface of activated carbon. High adsorption capacity values (q_{max}) from 214 to 275 mg/g were obtained in this study, higher than previous results of 30 mg/g [34] or 16–21 mg/g [37] for azorubine adsorption in activated carbon. cPAC showed the maximum adsorption capacity, related with its higher adsorption area. This effect of adsorption capacity with particle size is well documented [38].

3.3. Modelling adsorption kinetics of azorubine on activated carbons

Adsorption kinetics plots of q_t vs time for free GAC, μGAC and cPAC using an adsorbent concentration of 2 g/L and an azorubine

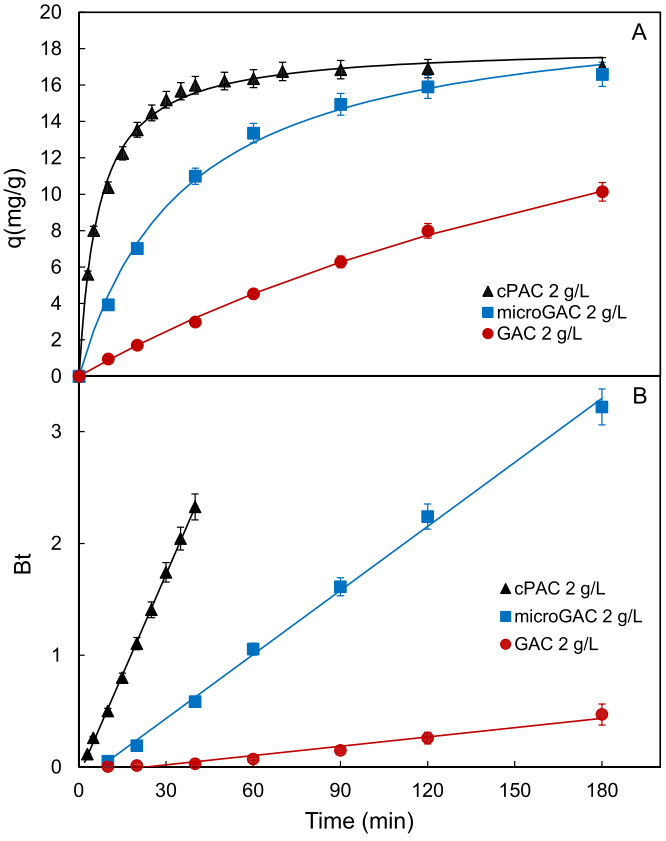

Fig. 5. Adsorption kinetic curves (A) and Boyd plot (B) of azorubine adsorption on free GAC, μGAC, cPAC, using a 2 g/L activated carbon concentration, and a flat blade stirring rate of 200 rpm.

concentration of 34 mg/L (pH 7.0) were modelled with pseudo-first order, pseudo-second order and Elovich models. Table 3 shows the kinetic constants obtained with these models. Although pseudo-first order and pseudo-second order models describe well data for GAC and μGAC, Fig. 5A shows the results of pseudo-second order model because its better fit for cPAC. Elovich model gives the lowest cPAC showed the higher adsorption rate versus μGAC and GAC, so it was selected for next

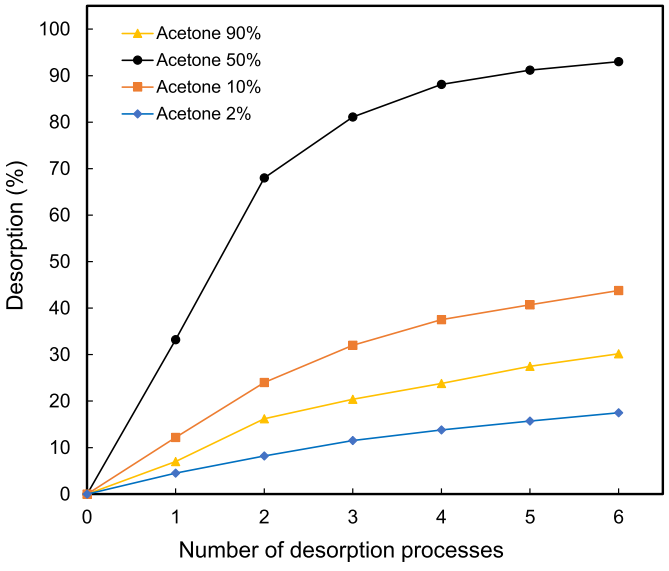

Fig. 6. Effect of different acetone concentrations on sequential desorption of azorubine saturated cPAC.

experiments correlation with all activated carbons. Azorubine adsorption was fast at the beginning of the process due to the availability of active sites on the exterior surface, and after the saturation of those active sites azorubine was adsorbed with a slower rate. Adsorption rate was strongly dependent on particle size, and while GAC took more than 720 min to adsorb all azorubine, μGAC needs about 180 min, and cPAC around 90 min. Values of kinetic constants increase following the order GAC < μGAC < cPAC. Prior studies of dyes adsorption on GAC showed also good fits of adsorption kinetics with these models, but pseudo-second order was always better [34–35,39–40]. The effect of increased adsorbate uptake rate of dyes in activated carbons with decreasing adsorbent particle size is also reported [41].

Boyd's model was applied to kinetic data to analyse which is the main rate limiting step, intraparticle diffusion or film diffusion. Fig. 5B shows that the plot of Boyd number versus time is linear for GAC, μGAC and cPAC, passing close to origin. It can be concluded that pore-diffusion is the rate controlling step during experiments, as could be expected from the high microporous structure of the activated carbon employed. Effective diffusion coefficient Di (cm^2/min) calculated from slopes were 1.60 10^{-6}, 1.09 10^{-6} and 8.55 10^{-7} cm^2/s, for GAC, μGAC, and cPAC, respectively. It means that higher pore diffusional problems are found with GAC, that are minimized in case of the smaller cPAC particles. A different diffusion model is the homogeneous surface diffusion model (HSDM) that use a surface diffusion coefficient (Ds). It assumes that internal mass transfer is only due to surface diffusion and that pore volume diffusion resistance is negligible. Boyd's effective intraparticle diffusion coefficient (Di) can be considered similar to the HSDM surface diffusion coefficient (Ds) whenever Boyd plot intercept the origin [30]. It can be concluded that adsorption is mainly controlled by the presence of micropores in the surface.

3.4. Reuse of activated carbon: adsorption/desorption studies

Desorption of azorubine is important to allow activated carbon reuse in the prototypes of spinning adsorber submerged filters that are studied afterwards. Experiments were done with cPAC at the highest concentration than can be achieved in prototypes of 25 g/L. Initial studies showed the effect of pH and solvents on desorption using 0.1 M HCl (pH 1), deionized water (pH 6.5), 0.1 M NaOH (pH 13), ethanol 96%, and acetone 10%. Final %desorption reached were 0, 3, 9.4, 2.8 and 12.2%, respectively. At pH 13 the anionic acid dye azorubine is desorbed because pH is higher than pH_{PZC} (9.7) and surface sites of cPAC are

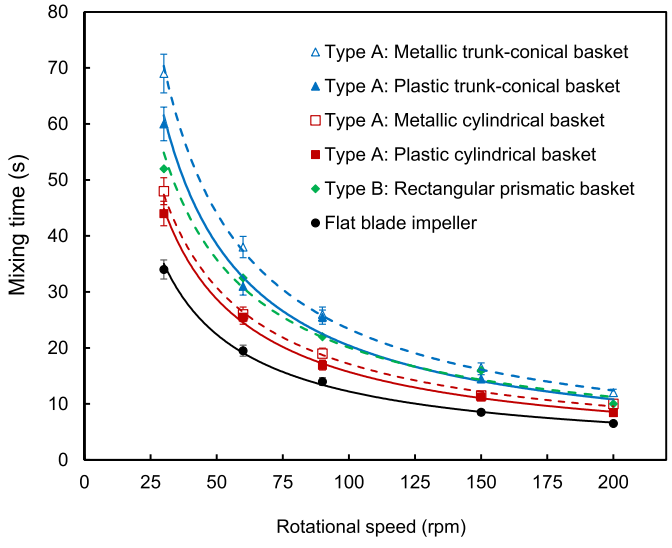

Fig. 7. Effect of basket configuration of spinning adsorbers on mixing times at different rotational speeds.

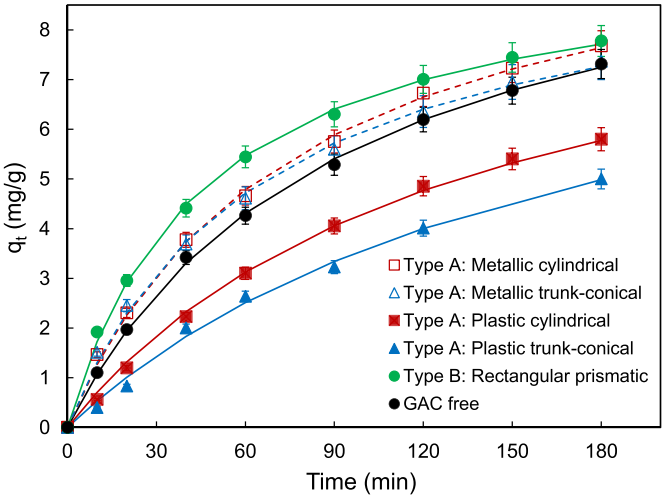

Fig. 8. Comparison of batch adsorption kinetic curves of azorubine obtained with different prototypes of spinning baskets adsorbers filled with GAC (4 g/L) and rotating at 200 rpm.

Table 4
Modelling parameters of adsorption kinetics with all adsorber prototypes studied filled with GAC 4 g/L.

Adsorber prototype	Pseudo-second order model parameters		
	k_2 (g/mg min)	q_e (mg/g)	r^2
Type A: metallic cylindrical	0.00121	10.88	0.999
Type A: metallic trunk-conical	0.00152	9.94	0.998
Type A: plastic cylindrical	0.00076	10.00	0.998
Type A: plastic trunk-conical	0.00058	9.83	0.995
Type B: metallic rectangular prismatic	0.00223	9.69	0.999
GAC free: flat blade impeller	0.00098	10.99	0.999

charged negatively. At pH 1.0 no desorption is observed. As expected, the interaction of the dye molecule and activated carbon is partially electrostatic. As the best %desorption was obtained with acetone 10%, a new experiment studied a sequential desorption process with different acetone concentrations (Fig. 6). A high desorption of 91.3% was reached after five desorption processes. Once azorubine was desorbed (94%) a new adsorption was done to evaluate cPAC reuse. A 65% of maximum adsorption was reached (175 mg/g), which means that a high azorubine amount can be adsorbed after cPAC reuse. Spinning adsorber submerged filters have cPAC confined helping for successive desorption/adsorption steps.

3.5. Prototyping spinning adsorbers: mixing time studies with empty baskets

Fig. 7 shows the effect of rotational speed of the different prototypes proposed in this study on mixing times. All spinning adsorbers showed higher mixing times in comparison with the flat blade impeller. In case of prototypes of spinning adsorbers type A that offers a radial flow pattern, the cylindrical basket configuration gives lower mixing times in comparison with the trunk-conical basket configuration. In addition, plastic basket configuration offers lower mixing times than metallic basket configuration. Spinning adsorber type B with an axial flow pattern offered mixing times between cylindrical and trunk-conical baskets and it is an intermediate option from the mixing time point of view. Running at the higher rotational speed of 200 rpm, mixing times are in the range from 7 to 12 s. Typical mixing times of stirred tanks using improved impeller designs are in the range from 3 to 6 s [42]. Flow regimes in mixing tanks depends on Reynolds number of impellers, and as an example the flat blade impeller of this study using rotational

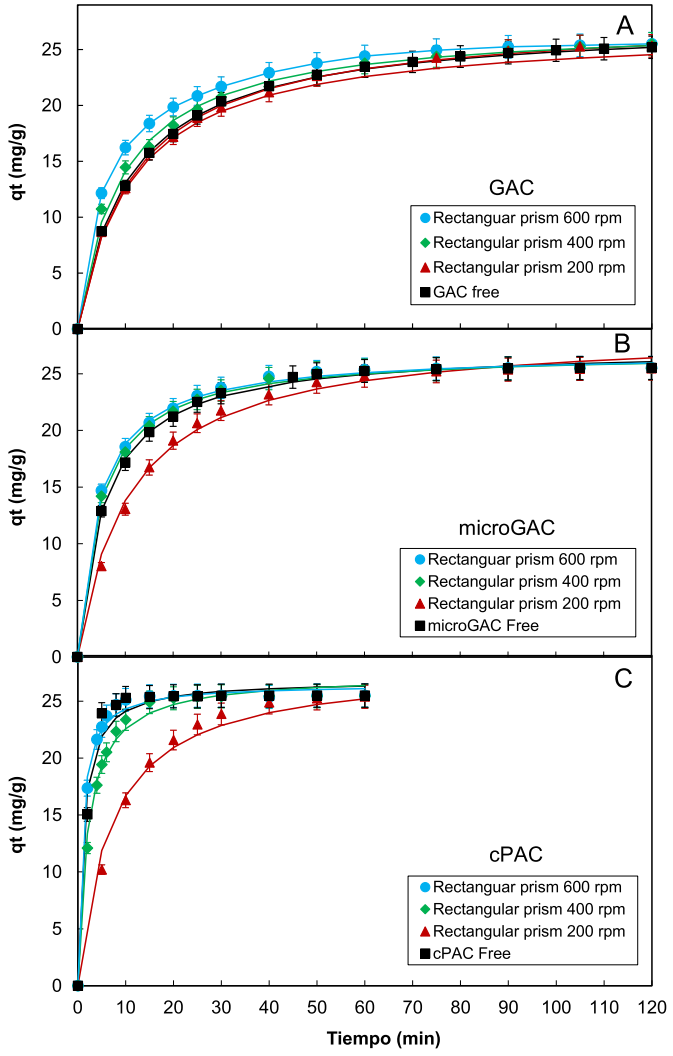

Fig. 9. Batch adsorption kinetic curves of azorubine obtained with a rectangular prismatic spinning adsorber filled with (A) GAC, (B) μGAC and (C) cPAC (25 g/L) at different rotating speeds.

Table 5
Pseudo-second order kinetic parameter obtained in a spinning rectangular prismatic prototype with GAC, μGAC, cPAC, at different rotation speeds.

Activated carbon	Parameter	Free	Adsorber rotation speed		
		200 rpm	200 rpm	400 rpm	600 rpm
GAC	k_2 (g/mg min)	0.00330	0.00303	0.00393	0.00557
	q_e (mg/g)	27.52	27.88	27.34	26.9
	r^2	0.999	0.999	0.996	0.998
μGAC	k_2 (g/mg min)	0.00659	0.00320	0.00805	0.00873
	q_e (mg/g)	27.27	28.78	26.91	26.87
	r^2	0.998	0.994	0.998	0.998
cPAC	k_2 (g/mg min)	0.03315	0.00523	0.01753	0.04263
	q_e (mg/g)	26.83	28.07	27.30	26.49
	r^2	0.979	0.988	0.991	0.994

speeds higher than 30 rpm run in a turbulent mixing regime with Reynolds numbers above 5000 [24]. Spinning adsorbers had to be run with a high rotational speed close to or higher than 200 rpm to reduce mixing times, minimize mass transfer limitations and then optimize adsorption rate.

3.6. Prototyping spinning adsorbers: selection of best basket geometry with GAC

Once studied the effect of rotational speed, the proposed spinning adsorbers prototypes were compared studying batch adsorption of an initial azorubine concentration of 34 mg/L (pH 7.0), GAC as adsorbent with a maximum load of 4 g/L, and a fixed rotational speed of 200 rpm. Results were compared with free GAC stirred with a flat bade impeller. Fig. 8 shows the adsorption kinetic plots obtained that fitted properly with the pseudo-second order kinetic model of Ho. Table 4 gives data of the calculated adsorption kinetic parameters. As expected, experiment with free GAC at 4 g/L gives faster adsorption kinetics than previous results with a lower adsorbent concentration of 2 g/L. Metallic prototypes with open mesh in all directions had faster adsorption kinetics than plastic ones, so it is essential to use this open mesh basket configuration to minimize mass transfer problems in the spinning adsorbers. Cylindrical geometry was preferred versus trunk-conical, and this effect is mainly observed with plastic prototypes. In case of metallic prototypes adsorption kinetics were faster than obtained with free GAC which means that the rotation of adsorbers minimize external mass transport and pore diffusion due to the internal flow inside the adsorbers. The best spinning adsorber prototype was the metallic open mesh rectangular prismatic configuration with axial flow pattern, and it was selected for further studies. In addition, this prototype can work with a higher adsorbent concentration of 25 g/L. The rectangular prismatic basket configuration type B offers an axial flow where flow enters mainly through the bottom side of the rectangular prism and then flow radially by the effect of centrifugal force. In contrast, spinning adsorbers type A offers a radial pattern flow where flows enter mainly through the side in contact with rotation and exits by the opposite direction [43].

These results are consistent with scientific literature that explore batch adsorption kinetics with different rotating basket geometries. A study with a rotating basket adsorber made with two cylindrical baskets of stainless-steel and filled with bone char of particle diameters higher than 0.79 mm reveals that external mass transport does not control adsorption rate at rotating speeds higher than 200 rpm [44]. A similar cylindrical basket adsorber that rotates with an additional impeller using activated carbon particles of 0.822 mm was operated at 700 rpm to minimize mass transport phenomena [45]. Another work uses a rotating

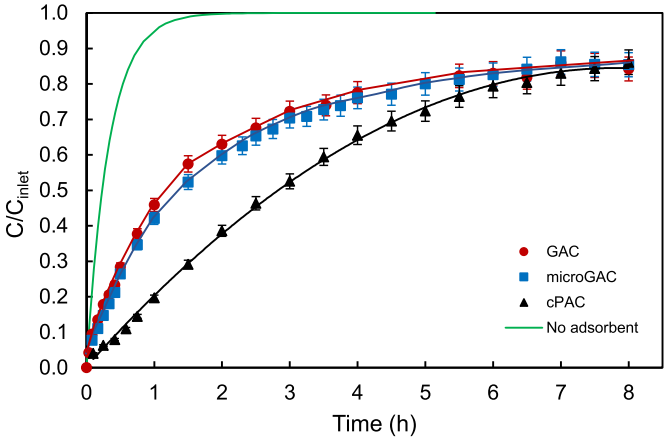

Fig. 10. Continuous operation of a rectangular prismatic spinning adsorber filled with GAC, μGAC, or cPAC (25 g/L), using an inlet azorubine concentration (Cinlet) of 500 mg/L, and t = 20 min.

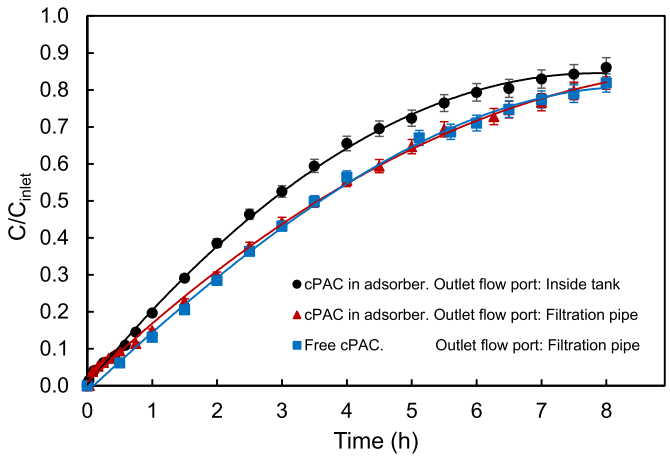

Fig. 11. Continuous operation of a rectangular prismatic adsorber (Cinlet = 500 mg/L, and t = 20 min) running as a submerged filter with confined (▲) or free cPAC (■), in comparison with operation with no filtration (●).

cylindrical basket adsorber for zinc removal with a cation exchange resin of 0.3–1.2 mm particle size and concludes that maximum adsorption kinetics were obtained at 400 rpm [46]. In reviewed cases open wired baskets were used with rotation speeds higher than 200 rpm and adsorbent particles of sizes higher than 0.3 mm. No data of mesh hole size of metallic baskets are found in reference papers.

3.7. Optimizing rotating speed of rectangular prismatic spinning adsorbers

Once selected the rectangular prismatic adsorber as the best prototype, new batch adsorption studies were done to evaluate the use of μGAC or cPAC using rotating speeds higher than 200 rpm. Fig. 9 compares the adsorption kinetics of spinning adsorbers filled with GAC, μGAC and cPAC that rotates at speeds from 200 to 600 rpm versus free GAC at 200 rpm. The used activated carbon dose was the maximum amount that avoid activated carbon compaction inside the adsorption unit. Activated carbon and azorubine concentrations studied were 25 g/L and 510 mg/L, respectively. Fig. 9A shows that spinning adsorber filled with GAC has adsorption kinetics similar or faster than free GAC even at the lower rotation speed of 200 rpm. However, in case of μGAC rotation speeds should be equal or higher than 400 rpm to get over kinetics of free μGAC (Fig. 9B). When cPAC is used only the higher rotating speed of 600 rpm offers adsorption kinetics as fast as free cPAC (Fig. 9C). The cPAC particles go from being compact to improving fluidization within the adsorber basket as stirring speed increases. The high rotation speed allows a good wetting efficiency of particles and mixing inside the spinning adsorbers. Table 5 shows the kinetic parameters obtained modelling with pseudo-second order adsorption kinetics. The initial adsorption rate of azorubine calculated as $k_2\ q_t^2$ for cPAC at 600 rpm was 29.9 mg/g min. The prismatic rectangular adsorber prototype rotating at 600 rpm and filled with cPAC (25 g/L) is the best prototype studied and can remove totally (99.8%) of azorubine in 15 min with no need of activated carbon separation.

3.8. Continuous flow operation of rectangular prismatic spinning adsorber as submerged filter

The prismatic rectangular prototype was selected to study continuous operation of spinning adsorbers rotating at 600 rpm with a 25 g/L activated carbon concentration. A high inlet azorubine concentration of 500 mg/L (pH 7.0) and a low hydraulic retention time of 20 min were selected to achieve maximum adsorption capacity of activated carbons in a short time. Fig. 10 shows initial continuous experiments done with outlet flow port located inside the tank. Adsorption rate of azorubine on GAC, μGAC and cPAC is compared with the use of no adsorbent. Maximum adsorption capacity of all activated carbons was achieved after 8 h, lowering considerably inlet azorubine concentration during operation. cPAC showed the higher adsorption rate versus μGAC and GAC, so it was selected for next experiments. There was no adsorbent loss during 8 h of continuous operation.

Final studies were done with cPAC using previous continuous operation conditions but with the spinning adsorber running as a submerged filter. It means that flow exits from the central axis (see Fig. 2) once filtered through the stainless-steel woven wire of 85 μm of mesh hole size. When the spinning adsorber run as a submerged filter filled with cPAC azorubine is always in contact with activated carbon before leaving the adsorber unit. A second option is to run the spinning adsorber submerged filter with free cPAC located inside the tank, instead of being confined in the spinning adsorber. Fig. 11 compares with previous experiments the evolution of azorubine concentration in the outlet flow using both configuration proposals of spinning adsorber submerged filter. Results shows faster adsorption rates running as a spinning adsorber submerged filter, so this configuration was chosen as the best. Values of adsorption rates with confined or free cPAC were similar, which means that confined cPAC adsorbs azorubine as fast as free cPAC. The high rotation speed allows a fast adsorption rate of azorubine when activated carbon is confined, and internal flow contributes to minimize diffusional problems. Rotation of the spinning adsorber also promotes a good mixture of the free cPAC located in tank, decrease the diffusion layer thickness that surrounds the particles, and minimize clogging problems that could arise during filtration. Thus, adsorption unit can run both with confined and free cPAC just as effectively. Visual observation proved that confined cPAC was fluidized within the filter and do not aggregate during experiment.

The high adsorption rates of azorubine obtained with the spinning adsorber unit confirm adsorption as one of the preferred techniques that can be used to purify industrial wastewater or to clean drinking water, versus other physical methods as nanofiltration or reverse osmosis [47]. The combination of low-pressure membrane processes as MF/UF with PAC adsorption is a recent trend to adsorb trace dissolved contaminants in wastewaters [48]. Different PAC dossing protocols and continuous PAC-membrane systems are proposed [49,50].

The adsorption unit proposed offer a novel opportunity for its application in wastewater treatments plants for removal of anionic azo dyes as azorubine or other micropollutans. An advantage is that the filters used in this work minimize clogging because of the high mesh hole size used (85 μm). Selection of best operation conditions for a specific configuration and water contaminant concentration requires further experimentation to optimize important variables of the adsorption unit as activated carbon concentration and hydraulic retention time.

4. Conclusions

A rectangular prismatic spinning submerged filter protype is proposed as the best adsorption unit for wastewater contaminants removal. Using azorubine as model contaminant it reached the highest removal efficiency of all studied prototypes. cPAC was selected as the best adsorbent versus GAC or μGAC, because its lower particle size (0.237 mm) increases adsorption area and minimize pore blocking. A high rotation speed of 600 rpm is needed to increase internal flow inside the adsorbent unit and minimize external and intraparticular diffusional problems. The rectangular prismatic spinning submerged filter protype with confined cPAC can be operated both in batch and continuous mode. In continuous mode it must be operated as a submerged filter with interesting advantages: (a) it allows increasing the concentration of activated carbon in the adsorption unit, since the entire volume of the tank can be filled with new adsorbent material, (b) the adsorbent can be progressively added by adjusting the dosage to the presence and concentration of adsorbate, (c) it is possible to combine two types of

adsorbent materials of different nature, one inside the tank and the other in the basket, which can be replaced independently, (d) the fast rotation of the submerged filter allows a good mixing of the adsorbent but also minimize filter clogging, (e) it could be used as a hybrid unit combining, for example, an advanced oxidation treatment with adsorption, (f) it can be used to remove all kind of contaminants selecting a good adsorbent with particle sizes ranging between 80 and 250 μm, and (g) saturated adsorbent can be regenerated in situ under batch operation using adequate solvents, acid, basic or saline solutions that favour contaminants desorption.

To get the best potential of this adsorber unit it is necessary to study applications on a large scale with real wastewaters from industrial or domestic effluents, adjusting the adsorbent dose and residence time needed to remove the concentration of contaminants present in wastewaters.

Declaration of competing interest

The authors declare that they have no known competing financial interests or personal relationships that could have appeared to influence the work reported in this paper.

Acknowledgements

We want to thank Hector Flores Aparicio (Industrial Design and Scientific Calculation Service, UPCT) for 3D printing of studied prototypes and useful suggestions.

Funding

This research did not receive any specific grant from funding agencies in the public, commercial, or not-for-profit sectors.

References

[1] B. Lellis, C.Z. Fávaro-Polonio, J.A. Pamphile, J.C. Polonio, Effects of textile dyes on health and the environment and bioremediation potential of living organisms, Biotechnol. Res. Innov. 3 (2019) 275–290, https://doi.org/10.1016/j.biori.2019.09.001.

[2] T. Rasheed, B. Bilal, F. Nabeel, M. Adeel, H.M.N. Iqbal, Environmentally-related contaminants of high concern: potential sources and analytical modalities for detection, quantification, and treatment, Environ. Int. 122 (2019) 52–66, https://doi.org/10.1016/j.envint.2018.11.038.

[3] Y. Tang, Y. Zhong, H. Li, Y. Huang, X. Guo, F. Yang, Y. Wu, Contaminants of emerging concern in aquatic environment: occurrence, monitoring, fate, and risk assessment, Water Environ. Res. 92 (2020) 1811–1817, https://doi.org/10.1002/wer.1438.

[4] T. Shindhal, P. Rakholiya, S. Varjani, A. Pandey, H.H. Ngo, W. Guo, H.Y. Ng, M. Taherzadeh, A critical review on advances in the practices and perspectives for the treatment of dye industry wastewater, Bioengineered 12 (2021) 70–87, https://doi.org/10.1080/21655979.2020.1863034.

[5] P.R. Rout, T.C. Zhang, P. Bhunia, R.Y. Surampalli, Treatment technologies for emerging contaminants in wastewater treatment plants: a review, Sci. Total Environ. 753 (2021), 141990, https://doi.org/10.1016/j.scitotenv.2020.141990.

[6] S. Dutta, B. Gupta, S.K. Srivastava, A.K. Gupta, Recent advances on the removal of dyes from wastewater using various adsorbents: a critical review, Mater. Adv. 2 (2021) 4497–4531, https://doi.org/10.1039/d1ma00354b.

[7] P. Moradihamedani, Recent advances in dye removal from wastewater by membrane technology: a review, Polym. Bull. (2021), https://doi.org/10.1007/s00289-021-03603-2.

[8] K. Kosek, A. Luczkiewicz, S. Fudala-Książek, K. Jankowska, M. Szopińska, O. Svahn, J. Tränckner, A. Kaiser, V. Langas, E. Björklund, Implementation of advanced micropollutants removal technologies in wastewater treatment plants (WWTPs) - examples and challenges based on selected EU countries, Environ. Sci. Policy 112 (2020) 213–226, https://doi.org/10.1016/j.envsci.2020.06.011.

[9] L. Liu, Z. Chen, J. Zhang, D. Shan, Y. Wu, L. Bai, B. Wang, Treatment of industrial dye wastewater and pharmaceutical residue wastewater by advanced oxidation processes and its combination with nanocatalysts: a review, J. Water Process Eng. 42 (2021) 10212, https://doi.org/10.1016/j.jwpe.2021.102122.

[10] V. Vaiano, O. Sacco, G. Libralato, G. Lofrano, A. Siciliano, F. Carraturo, M. Guida, M. Carotenuto, Degradation of anionic azo dyes in aqueous solution using a continuous flow photocatalytic packed-bed reactor: influence of water matrix and toxicity evaluation, J. Environ. Chem. Eng. 8 (2020), 104549, https://doi.org/10.1016/j.jece.2020.104549.

[11] R. Rashid, I. Shafiq, P. Akhter, M.J. Iqbal, M. Hussain, A state-of-the-art review on wastewater treatment techniques: the effectiveness of adsorption method, environ sciPollut. Res. 28 (2021) 9050–9066, https://doi.org/10.1007/s11356-021-12395-x.

[12] N.U.M. Nizam, M.M. Hanafiah, E. Mahmoudi, A.A. Halim, A.W. Mohammad, The removal of anionic and cationic dyes from an aqueous solution using biomass-based activated carbon, Sci. Rep. 11 (2021) 8623, https://doi.org/10.1038/s41598-021-88084-z.

[13] S. Yadav, A. Yadav, N. Bagotia, A.K. Sharma, S. Kumar, Adsorptive potential of modified plant-based adsorbents for sequestration of dyes and heavy metals from wastewater - a review, J. Water Process Eng. 42 (2021), 102148, https://doi.org/10.1016/j.jwpe.2021.102148.

[14] A.M. Awad, S.M.R. Shaikh, R. Jalab, M.H. Gulied, M.S. Nasser, A. Benamor, S. Adham, Adsorption of organic pollutants by natural and modified clays: a comprehensive review, Sep. Purif. Technol. 228 (2019) 11571, https://doi.org/10.1016/j.seppur.2019.115719.

[15] S.F. Chua, A. Nouri, W.L. Ang, E. Mahmoudi, A.W. Mohammad, A. Benamor, M. Ba-Abbad, The emergence of multifunctional adsorbents and their role in environmental remediation, J. Environ. Chem. Eng. 9 (2021), 104793, https://doi.org/10.1016/j.jece.2020.104793.

[16] M.B. Mosbah, L. Mechi, R. Khiari, Y. Moussaoui, Current state of porous carbon for wastewater treatment, Processes 8 (2020) 1651, https://doi.org/10.3390/pr8121651.

[17] A.A. Siyal, M.R. Shamsuddin, A. Low, N.E. Rabat, A review on recent developments in the adsorption of surfactants from wastewater, J. Environ. Manag. 254 (2020), 109797, https://doi.org/10.1016/j.jenvman.2019.109797.

[18] D.D. Ratnayaka, M.J. Brandt, K.M. Johnson, Specialized and advanced water treatment processes, in: D.D. Ratnayaka, M.J. Brandt, K.M. Johnson (Eds.), Water Supply, Sixth edition, Butterworth-Heinemann, 2009, pp. 365–423, https://doi.org/10.1016/B978-0-7506-6843-9.00018-4.

[19] V. Kårelid, G. Larsson, B. Björlenius, Pilot-scale removal of pharmaceuticals in municipal wastewater: comparison of granular and powdered activated carbon treatment at three wastewater treatment plants, J. Environ. Manag. 193 (2017) 491–502, https://doi.org/10.1016/j.jenvman.2017.02.042.

[20] P.D. Nguyen, T.M.T. Le, T.K.Q. Vo, P.T. Nguyen, T.D.H. Vo, B.T. Dang, N.T. Son, D. D. Nguyen, X.T. Bui, Submerged membrane filtration process coupled with powdered activated carbon for nonylphenol ethoxylates removal, Water Sci. Technol. 84 (2021) 1793–1803, https://doi.org/10.2166/wst.2021.380.

[21] Y.S. Ng, Y.T. Tan, A.S.M. Chua, M.A. Hashim, B.S. Gupta, Removal of nickel from water using rotating packed bed contactor: parametric studies and mode of operations, J. Water Process Eng. 36 (2020), 101286, https://doi.org/10.1016/j.jwpe.2020.101286.

[22] M.E. Ossman, M. Abdelfatah, Y. Kiros, Preparation, characterization and adsorption evaluation of old newspaper fibres using basket reactor (Nickel removal by Adsorption), Int. J. Environ. Res. 10 (2016) 119–130. https://doi.org/10.22059/IJER.2016.56894.

[23] H.K. Larsson, P.A.S. Andersen, E. Byström, K. Gernaey, U. Krühne, CFD modeling of flow and ion exchange kinetics in a rotating bed reactor system, Ind. Eng. Chem. Res. 56 (2017) 3853–3865, https://doi.org/10.1021/acs.iecr.7b00224.

[24] T. Menisher, M. Metghalchi, E.B. Gutoff, Mixing studies in bioreactors, Bioprocess Eng. 22 (2000) 115–120, https://doi.org/10.1007/s004490050020.

[25] P. Sinha, A. Datar, C. Jeong, X. Deng, Y.G. Chung, L.C. Lin, Surface area determination of porous materials using the Brunauer–Emmett–Teller (BET) method: limitations and improvements, J. Phys. Chem. C 123 (2019) 20195–20209, https://doi.org/10.1021/acs.jpcc.9b02116.

[26] N. Fiol, I. Villaescusa, Determination of sorbent point zero charge: usefulness in sorption studies, Environ. Chem. Lett. 7 (2009) 79–84, https://doi.org/10.1007/s10311-008-0139-0.

[27] G. McKay, A. Mesdaghinia, S. Nasseri, M. Hadi, M.S. Aminabad, Optimum isotherms of dyes sorption by activated carbon: fractional theoretical capacity & error analysis, Chem. Eng. J. 251 (2014) 236–247, https://doi.org/10.1016/j.cej.2014.04.054.

[28] M.A. Al-Ghouti, D.A. Da'ana, Guidelines for the use and interpretation of adsorption isotherm models: a review, J. Hazard. Mater. 393 (2020), 122383, https://doi.org/10.1016/j.jhazmat.2020.122383.

[29] G. León, F. García, B. Miguel, J. Bayo, Equilibrium, kinetic and thermodynamic studies of methyl orange removal by adsorption onto granular activated carbon, Desalin. Water Treat. 57 (2016) 17104–17117, https://doi.org/10.1080/19443994.2015.1072063.

[30] R.M.C. Viegas, M. Campinas, H. Costa, M.J. Rosa, How do the HSDM and Boyd's model compare for estimating intraparticle diffusion coefficients in adsorption processes, Adsorption 20 (2014) 737–746, https://doi.org/10.1007/s10450-014-9617-9.

[31] F. Güzel, Z. Tez, The characterization of the micropore structures of some activated carbons of plant origin by N2 and CO2 adsorptions, Sep. Sci. Technol. 28 (1993) 1609–1627, https://doi.org/10.1080/01496399308018061.

[32] F. Duarte, F.J. Maldonado-Hódar, L.M. Madeira, Influence of the characteristics of carbon materials on their behaviour as heterogeneous Fenton catalysts for the elimination of the azo dye Orange II from aqueous solutions, Appl. Catal. B. 103 (2011) 109–115, https://doi.org/10.1016/j.apcatb.2011.01.016.

[33] C. Andriantsiferana, C. Julcour-Lebigue, C. Creanga-Manole, H. Delmas, A.-M. Wilhelm, Competitive adsorption of p-hydroxybenzoic acid and phenol on activated carbon: experimental study and modeling, J. Environ. Eng. 139 (2013) 402–409, https://doi.org/10.1061/(ASCE)EE.1943-7870.0000600.

[34] C. Valderrama, J.L. Cortina, A. Farran, V. Marti, X. Gamisans, F.X. de las Heras, Characterization of azo dye (Acid Red 14) removal with granular activated carbon:

equilibrium and kinetic data, Solvent Extr. Ion Exch. 26 (2008) 271–288, https://doi.org/10.1080/07366290802053504.
[35] M.T. Yagub, T.K. Sen, S. Afroze, H.M. Ang, Dye and its removal from aqueous solution by adsorption: a review, Adv. Colloid Interf. Sci. 209 (2014) 172–184, https://doi.org/10.1016/j.cis.2014.04.002.
[36] K.K.H. Choy, J.F. Porter, G. Mckay, Film-surface diffusion during the adsorption of acid dyes onto activated carbon, Chem. Eng. J. 103 (2004) 133–145, https://doi.org/10.1016/j.cej.2004.05.012.
[37] A. Haji, N.M. Mahmoodi, Soy meal hull activated carbon: preparation, characterization and dye adsorption properties, Desalin. Water Treat. 44 (2012) 237–244. https://doi.org/10.5004/dwt.2012.3104.
[38] E.N. El Qada, S.J. Allen, G.M. Walker, Adsorption of Methylene Blue onto activated carbon produced from steam activated bituminous coal: a study of equilibrium adsorption isotherm, Chem. Eng. J. 124 (2006) 103–110, https://doi.org/10.1016/j.cej.2006.08.015.
[39] V. Gómez, M.S. Larrechi, M.P. Callao, Kinetic and adsorption study of acid dye removal using activated carbon, Chemosphere 69 (2007) 1151–1158, https://doi.org/10.1016/j.chemosphere.2007.03.076.
[40] B. Hayati, N.M. Mahmoodi, Modification of activated carbon by the alkaline treatment to remove the dyes from wastewater: mechanism, isotherm and kinetic, Desalin. Water Treat. 47 (2012) 322–333, https://doi.org/10.1080/19443994.2012.696429.
[41] X. Yang, B. Al-Duri, Kinetic modeling of liquid-phase adsorption of reactive dyes on activated carbon, J. Colloid Interface Sci. 287 (2005) 25–34, https://doi.org/10.1016/j.jcis.2005.01.093.
[42] J.M. Grau, J.M. Bisang, Mass transfer studies at packed bed rotating cylinder electrodes of woven-wire meshes, J. Appl. Electrochem. 36 (2006) 759–763, https://doi.org/10.1007/s10800-006-9125-z.
[43] T. Kumaresan, J.B. Joshi, Effect of impeller design on the flow pattern and mixing in stirred tanks, Chem. Eng. J. 115 (2006) 173–193, https://doi.org/10.1016/j.cej.2005.10.002.
[44] R. Leyva-Ramos, J. Rivera-Utrilla, N.A. Medellin-Castillo, M. Sanchez-Polo, Kinetic modeling of fluoride adsorption from aqueous solution onto bone char, Chem. Eng. J. 158 (2010) 458–467, https://doi.org/10.1016/j.cej.2010.01.019.
[45] C.-F. Chang, S.-C. Lee, Adsorption behavior of pesticide methomyl on activated carbon in a high gravity rotating packed bed reactor, Water Res. 46 (2012) 2869–2880, https://doi.org/10.1016/j.watres.2012.02.041.
[46] O. Abdelwahab, N.K. Amin, E.-S.Z. El-Ashtoukhy, Removal of zinc ions from aqueous solution using a cation exchange resin, Chem. Eng. Res. Des. 91 (2013) 165–173, https://doi.org/10.1016/j.cherd.2012.07.005.
[47] V. Katheresan, J. Kansedo, S.-Y. Lau, Efficiency of various recent wastewater dye removal methods: a review, J. Environ. Chem. Eng. 6 (2018) 4676–4697, https://doi.org/10.1016/j.jece.2018.06.060.
[48] J. Löwenberg, T. Wintgens, PAC/UF processes: current application, potentials, bottlenecks and fundamentals: a review, Crit. Rev. Env. Sci. Technol. 47 (2017) 1783–1835, https://doi.org/10.1080/10643389.2017.1382260.
[49] C. Campos, B.J. Mariñas, V.L. Snoeyink, I. Baudin, J.M. Lainé, PAC-membrane filtration process. II. Model application, J. Environ. Eng. 162 (2000) 104–111, https://doi.org/10.1061/(ASCE)0733-9372(2000)126:2(104).
[50] S. Chang, T.D. Waite, A.G. Fane, A simplified model for trace organics removal by continuous flow PAC adsorption/submerged membrane processes, J. Membr. Sci. 253 (2005) 81–87, https://doi.org/10.1016/j.memsci.2004.12.027.